

# A Helical Air-core Transformer with Even Current Distribution for VHF Converters \*

Jiahua Xu<sup>1</sup>, Zhiliang Zhang<sup>1</sup>, Xinlu Chen<sup>2</sup>, Ke Xu<sup>1</sup>, Zhou Dong<sup>1</sup>, and Xiaoyong Ren<sup>1</sup>

Aero-Power Sci-Tech Center, Nanjing University of Aeronautics and Astronautics, Nanjing, Jiangsu, P. R. China<sup>1</sup>

Beijing Century Goldray Semiconductor Co., Ltd<sup>2</sup>

{xujh0212, zlzhang, xuke, bigzhou, renxy}@nuaa.edu.cn

**Abstract**—Very High Frequency (VHF) converters allow the use of the air-core transformers owing to small required inductance. The traditional air-core transformers suffer from uneven current distribution caused by the proximity effect, which results in serious AC conduction loss. A new helical air-core transformer structure with even current distribution is proposed. In the proposed structure, all layers of windings with the same size are completely overlapped to reduce eddy current loss. The layer internal distance of overlapping PCB windings is adjusted to realize the desired transformer parameters. A 30 MHz GaN flyback converter with the PCB fabrication air-core transformer was built. With 15 V input and 15 V/ 21 W output, the proposed transformer structure improves the efficiency from 75.9% using the conventional transformer to 82.7% (an improvement of 6.8%). With 15 V input and 15 V/ 24 W output, the efficiency of the proposed transformer realizes 82.7%.

**Keywords**—air-core transformer; helical winding; Very high frequency (VHF); eGaN; HEMT; resonant converter

## I. INTRODUCTION

Very High Frequency (VHF, 30MHz-300MHz) converters with high efficiency, high power density and fast dynamic response have become promising in low power applications in recent years [1]-[3]. The dramatic increase of switching frequency greatly reduces the resonant component value to buffer energy so that the air-core transformers can be applied to VHF converters owing to its small inductance value [4].

The air-core transformers in low power applications have many advantages [5]. First, the air-core transformers without bulky magnetic cores can realize lightweight and miniaturization of the converters in favor of integration. Secondly, the air-core transformers are built with multi-layer Printed Circuit Boards (PCBs), which are convenient to realize mass manufacturing and parameter consistency. Additionally, the air-core transformers do not suffer high frequency core loss, saturation problem and other nonlinear drawbacks due to the magnetic component. However, the air-core transformers have the drawbacks of low inductance and coupling coefficient without magnetic material.

The air-core transformers can be implemented in various winding structures with different geometries, such as the spiral structure in [6][7] and the helical structure in [8]. Two structures are compared carefully in [9]. The conclusion is that with the same volume, the helical structure can achieve higher efficiency. However, a serious problem of imbalance current

distribution due to eddy current in the section of the helical transformer winding still causes considerable AC loss.

In this paper, a new helical air-core transformer structure with even current distribution is proposed, which helps to reduce eddy current loss and improve the utilization of windings. In the proposed structure, all layers of the windings with the same size are completely overlapped to reduce eddy current and the internal distance between the layers is adjusted to realize the desired transformer parameters.

## II. CHALLENGES OF IMPROVING AIR-CORE TRANSFORMER EFFICIENCY IN VHF CONVERTERS

### A. VHF Resonant Flyback Converter with SR

In order to test the performance of the air-core transformers, a 30 MHz resonant flyback converter based on GaN is designed, shown in Fig. 1. The converter consists of the class E inverter, the class E rectifier and the air-core transformer. The transformer absorbs the inductance  $L_{\sigma 1}$ ,  $L_{M1}$  and  $L_{\sigma 2}$  without additional inductors, which simplifies the circuit and reduces the volume. The digital ON/OFF control and synchronous rectifier technology is applied in the converter. The following analysis, transformer design and experimental verification are regarding to the converter shown in Fig. 1. The converter specifications are listed in Table I.

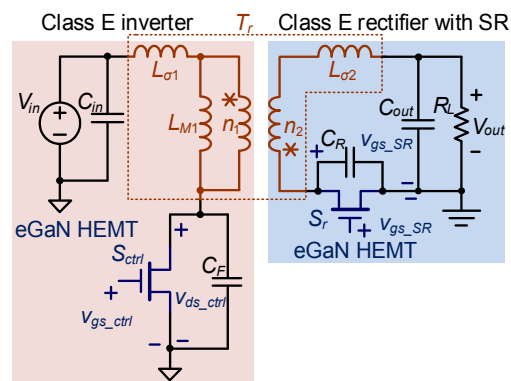


Fig. 1. VHF Class E resonant flyback converter

Table I CONVERTER SPECIFICATIONS

$V_{IN}$	$V_o$	$I_o$	$P_o$	$f_s$
15 V	15 V	1.6 A	24W	30 MHz

\*The work was supported by National Natural Science Foundation of China (51722702, 51377077), Outstanding Youth Fund of Jiangsu Province.

## B. Uneven Current Distribution in Helical Air-core Transformers

Although the air-core transformers have many advantages such as no core loss, small size and low weight in VHF converters, the helical winding structure widely used at present still has the problem of uneven current distribution. Fig. 2 shows a conventional PSSP (two primary layers respectively at the top and the bottom, and two secondary layers between two primary layers) helical transformer and the mechanism of its uneven current distribution. The density of the cross and the point represents the current density in Fig. 2. The current is concentrated in the overlapping area of the winding and only little current flows through the non-overlapping areas of the winding.

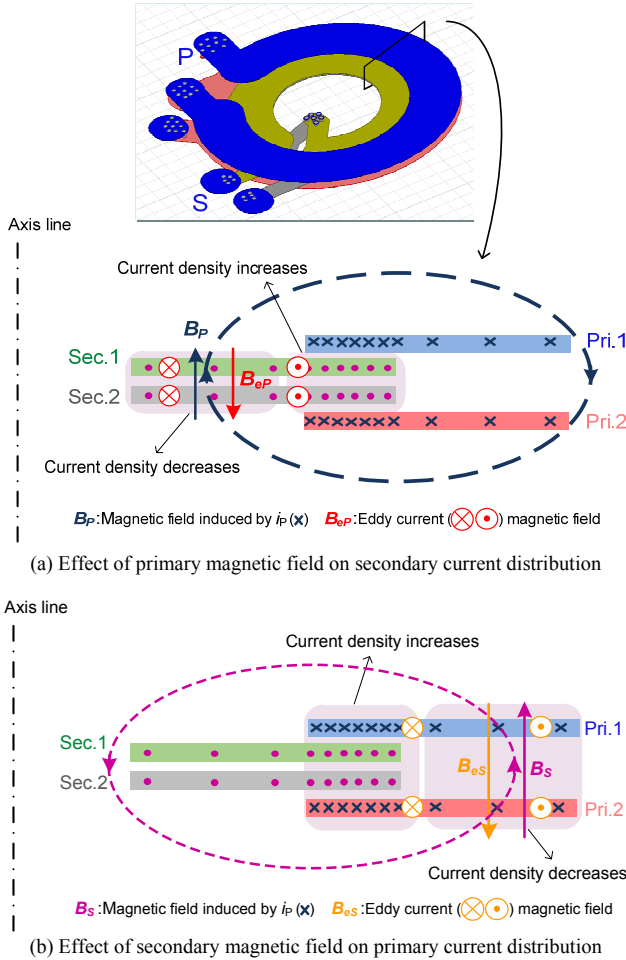


Fig. 2. Current distribution mechanism of conventional PSSP helical transformer

The mechanism of current distribution is based on the proximity effect. The detailed mechanism analysis is as follows. On the one hand, as seen from Fig. 2 (a), the primary current  $i_p$  travels inward, inducing an upward magnetic field  $B_P$  across the inner side of the secondary winding. The copper there effectively shields the flux path. A downward magnetic flux is needed to counteract  $B_P$ . Then the eddy current is generated in the copper of the inner secondary winding, which causes a current density decrease of the secondary current  $i_s$ ,

traveling outward in the inner secondary winding, and a current density increase of  $i_s$  in the winding overlapping area.

On the other hand, as shown in Fig. 2 (b), the secondary current  $i_s$  induces an upward magnetic field  $B_S$  across the outside of the primary winding. A downward eddy current magnetic field is generated to counteract the effect of  $B_S$  in the outer primary winding similarly. The resulting eddy current causes a current density increase of  $i_p$ , travelling inward in the winding overlapping area, and a current density decrease of  $i_p$  in the outer primary winding.

Fig. 3 shows the current distribution in the cross section of the conventional PSSP helical transformer. The transformer is simulated in ANSYS Maxwell software. The current density is high in the overlapping area of the windings and low in the non-overlapping area, which causes low utilization of the winding and large eddy current loss.

In general, the essential reason of uneven current distribution is that the magnetic induction line induced by the winding current impinges on the copper surfaces of the non-overlapping areas of the winding, and induces the eddy current there, leading to serious high loss and reduced inductance.

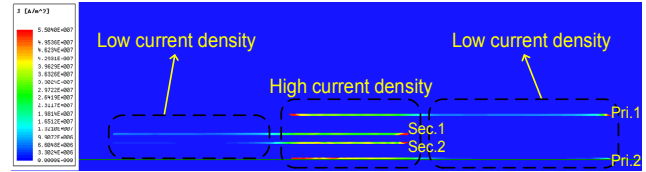


Fig. 3. Current distribution in cross section of conventional PSSP helical transformer ( $L_{11}=40$  nH,  $L_{22}=52$  nH,  $L_M=36$  nH,  $f=30$  MHz)

In summary, uneven current distribution in the helical air-core transformers is a problem to be solved. How to improve the ratio of winding utilization and decrease AC loss have become a challenge in designing air-core transformers.

## III. PROPOSED HELICAL AIR-CORE TRANSFORMER WITH EVEN CURRENT DISTRIBUTION

### A. Basic Idea of Proposed Helical Air-core Transformer

From the above analysis on the mechanism of uneven current distribution in the conventional helical windings, the reason of high eddy current is concluded as the copper layer shielding the flux path caused by inconsistency of each layer size. The basic idea of the proposed helical air-core transformer is to use the windings with completely overlapped layers of the same geometry and adjust the internal distance between the layers to realize the desired transformer parameters.

The conventional helical winding achieves higher efficiency than the spiral winding because less copper area is impinged on by the magnetic field lines. The efficiency of the helical transformers can be further improved in the same way. If the size of each layer is exactly the same, the magnetic flux formed by one winding have little influence on the other winding due to a complete overlap in all layers. However, once the geometry of the windings is fixed exactly as the same, the

inductance value cannot be adjusted flexibly and the design of the transformer can only achieve specific parameters.

The improved helical transformer requires to avoid copper area shielding the flux path and realize flexible parameter design. Through the use of windings with the same geometry, the optimization of the air-core helical transformer is translated to finding a way to adjust the inductance value flexibly when the coil geometry is fixed. Changing the distance between layers is just another way to adjust inductance value of windings in addition to adjusting the size of each layer. The magnetic coupling coefficient of the transformer decreases as the vertical distance between the arbitrary two layers increases. According to this, a new helical air-core transformer structure is proposed.

Fig. 4 shows the cross section of the proposed helical transformer. The helical structure uses multiple layers of a PCB and places each successive turn of a winding on the next layer of the board. The trace width and radii of all coils are the same and each layer of windings are completely superposed. The difference is that the distances between every two adjacent layers of the windings are adjustable. In the design example,  $d_2$  and  $d_3$  are set to the default thickness of the PCB dielectric layer (0.153 mm) and  $d_1$  is the variable. The first primary layer is one PCB, the other primary layer and the secondary winding compose another PCB. Once the geometry of each layer and the turns ratio are fixed,  $d_1$  is the only variable to adjust the transformer parameters. In the proposed helical structure, the magnetic field induced by the winding current traverse the air inside and outside the round coils without impinging on the copper area. The eddy current is dramatically reduced and the winding current is evenly distributed.

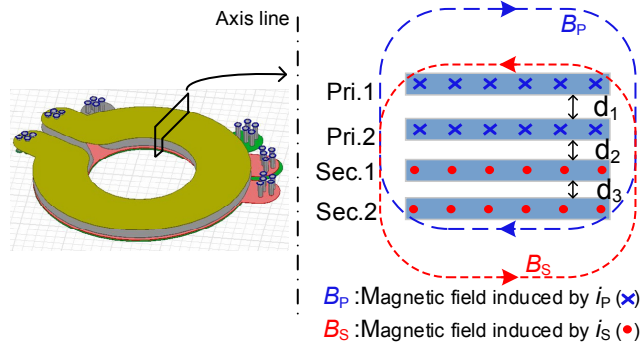


Fig. 4. Proposed helical transformer

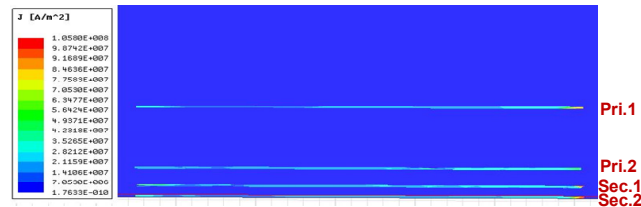


Fig. 5. Even current distribution in cross section of proposed helical transformer ( $L_{11}=56.1$  nH,  $L_{22}=59.7$  nH,  $L_M=45.8$  nH,  $f=30$  MHz)

Fig. 5 shows current distribution in the cross section of the proposed helical air-core transformer with PPSS structure (two primary layers at the top and two secondary layers at the bottom) simulated in ANSYS Maxwell. The current flowing

through the windings is basically evenly distributed, which greatly improves the utilization of windings. The influence of eddy current on transformer efficiency is greatly weakened. The general efficiency of the converter will increase with the decrease of AC conduction loss in the new helical air-core transformer.

Therefore, the thickness of the proposed helical air-core transformer need to be considered, which is slightly higher than the thickness of the conventional one. The increase in thickness directly influences the volume of the transformer. Fortunately, this increase is limited to about one millimeter or less, which can be ignored compared with the thickness of the converter.

The proposed transformer has the same constraint as the conventional helical one. That is the turns of the helical transformer are limited by the layers of PCB. Each additional turn means an additional PCB layer. If the required inductance value of the transformer is larger than a few tens of nanohenries, the number of PCB layers may be more than four layers, which will increase the difficulty and cost of production. Therefore, the operating frequency must be high (several tens MHz) to reduce energy storage requirement so that a few tens of nanohenries is enough for the converter. The converter in this paper operates at a frequency of 30 MHz, which makes it possible to design transformers in a standard 4-layer PCB process.

#### B. Design Procedures of Proposed Helical Transformer

The design of the proposed helical air-core transformer need to ensure the accuracy of the parameters. So it is necessary to realize the accurate calculation of the coil inductance. The computational formulas of the self inductance and mutual inductance are given in [10].

The T transformer model is shown in Fig. 6, where  $L_{\sigma 1}$  and  $L_{\sigma 2}$  are the leakage inductance of the primary and secondary windings,  $L_{M1}$  is the primary excitation inductance, and  $n_1$  and  $n_2$  are the turns of the primary and secondary coils. This model is used for the design of the converter shown in Fig. 1. The general idea of the air-core transformer design is listing the possible geometries through enumeration and selecting the ones with the desired parameters with the MATLAB script to constitute the transformer. The design procedures of proposed helical air-core transformers are as follows.

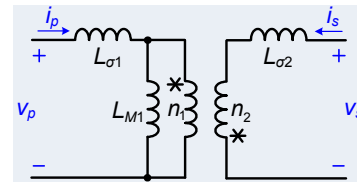


Fig. 6. T transformer model

First, solve the transformer parameters through the design of the converter. The self-inductance of the primary and secondary coil respectively  $L_{11}$ ,  $L_{22}$  and the mutual inductance  $L_M$  can be determined as

$$\begin{bmatrix} v_p \\ v_s \end{bmatrix} = \begin{bmatrix} L_{11} & L_M \\ L_M & L_{22} \end{bmatrix} \begin{bmatrix} i_p \\ i_s \end{bmatrix} \quad (1)$$

$$L_{11} = L_{\sigma 1} + L_{M1} \quad (2)$$

$$L_{22} = L_{\sigma 2} + \left(\frac{n_2}{n_1}\right)^2 L_{M1} \quad (3)$$

$$L_M = \left(\frac{n_2}{n_1}\right) L_{M1} \quad (4)$$

Then suppose the distance between the primary layers are adjustable and the distances between other two adjacent layers are set to the default thickness of the PCB dielectric layer. Enumerate trace width range and radius of the coil and sweep among the size range to obtain the geometries with the desired parameter  $L_{22}$ . The width and radius of the primary winding are fixed the same with the secondary winding.

Finally, adjust the distance between two primary layers of all coil solutions in the above step and select the optimal solution with the parameters  $L_{11}$ ,  $L_M$  approaching to the desired ones. In this way, the proposed helical air-core transformer is designed. The designed transformer is simulated in the finite element analysis software ANSYS Maxwell and slight adjustments in the dimension parameters are made according to the simulation results to verify the accuracy of the parameters.

### C. Design Example of Proposed Helical Transformer

To verify the effect of structural improvements on the helical air-core transformer efficiency, a conventional transformer and a proposed one with similar parameters are designed.

The designed 2:2 conventional helical transformer is shown in Fig. 7. The primary and secondary windings respectively comprise 2 circular turns connected in series, one turn in each layer. With two secondary layers at the top and two primary layers at the bottom of the PCB, it is called SSPP structure. The two primary layers have the same geometry and the two secondary layers are the same. It is noted that the thickness of the PCB is 0.60 mm.

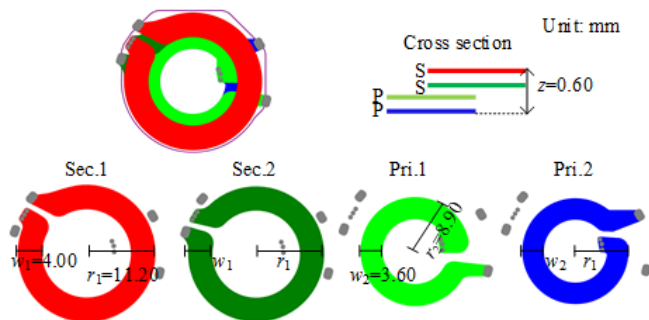


Fig. 7. Conventional helical transformer

The proposed helical air-core transformer is shown in Fig. 8 and Fig. 9. Similarly, the structure has four layers with the same geometry, one turn in each layer, with every 2 circular turns connected in series respectively for the primary and secondary windings. The distance between two primary layers

is 0.92 mm and the PCB thickness is 2.14 mm, which is higher than the conventional one. High temperature resistant plastic slices and glue are used to fabricate the spacing between two PCBs. Vernier caliper is used for measurements to make the spacing as close as possible to the design value.

The copper thickness of each layer in both transformers is selected to be 35  $\mu\text{m}$  (1 oz) as a trade-off between the copper loss and the cost. The primary and secondary windings of the conventional transformer have different geometries while the proposed transformer has an adjustable distance between two primary layers. The design of two transformers target at achieving the same coupling and self inductances to make it convenient and intuitive for performance comparison. The detailed parameters of two transformers are similar, as is given in Table II.

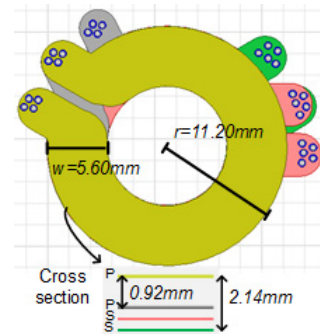


Fig. 8. Size of proposed helical transformer

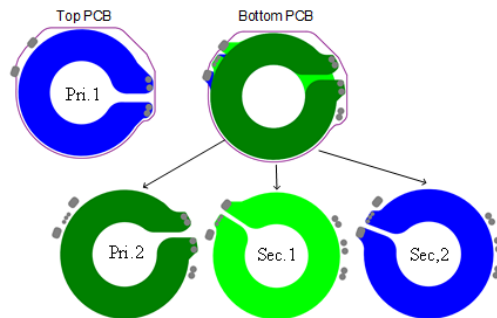


Fig. 9. Layer structure of proposed helical transformer

Table II TRANSFORMER PARAMETERS (UNIT: nH)

	Conventional	Proposed
$L_{11}$	59.0	56.1
$L_{22}$	63.3	59.7
$L_M$	48.5	45.8

The AC resistances of the two transformers obtained by the ANSYS Maxwell simulation are given in Table III. In general, with similar specifications, the AC resistances of the proposed transformer are comparatively lower, which directly reduces copper loss.

Table III AC RESISTANCE COMPARISON (UNIT:  $\Omega$ )

		30 MHz	60 MHz	90 MHz
Conventional transformer	Primary	0.122	0.173	0.212
	Secondary	0.187	0.265	0.325
Proposed transformer	Primary	0.113	0.160	0.196
	Secondary	0.119	0.169	0.207

#### IV. EXPERIMENTAL RESULTS AND DISCUSSION

In order to compare the performance of the two designed transformers, two 30 MHz resonant flyback prototypes are built to verify the optimization of transformer structure. The prototype of the converter including the front view and the side view is shown in Fig. 10. The assembly of the testing converter including the control stage and the power stage is shown in Fig. 11. The size specification of the converter is 33.5×50.0 mm with 3.0 mm thick. The component value of the power stage is given in Table IV.

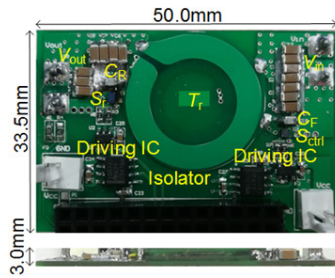


Fig. 10. Prototype of the converter

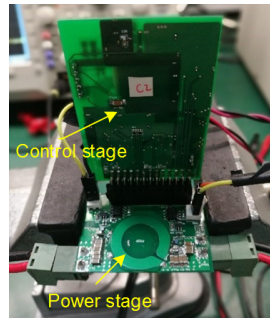


Fig. 11. Testing converter assembly

Table IV POWER STAGE COMPONENT VALUE

$S_{ctrl}$		EPC2039 (EPC, 80V, 6.8A)	
$S_r$		EPC2007C (EPC, 100V, 6A)	
$n_1$	2	$C_{in}$	10 $\mu$ F×7 (Murata)
$n_2$	2	$C_{out}$	10 $\mu$ F×10 (Murata)
$C_F$		160 pF (AVX)	
		$C_R$	180 pF (AVX)
		Conventional transformer	
$L_{\sigma 1}$	10.5 nH	Proposed transformer	
$L_{M1}$	48.6 nH		
$L_{\sigma 2}$	14.8 nH		

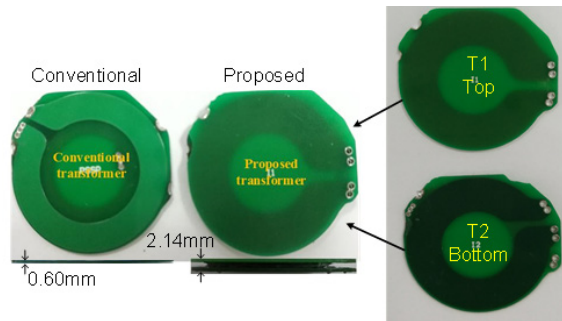
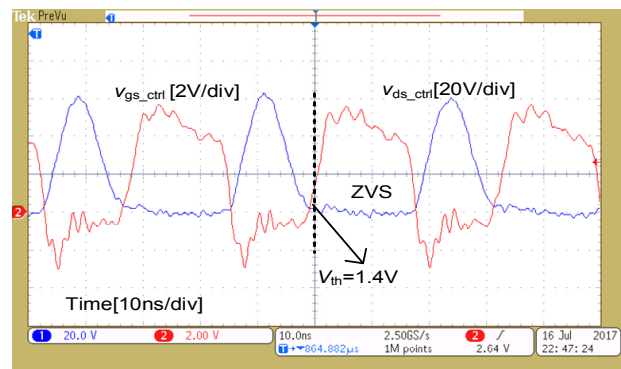


Fig. 12. Prototype of transformers

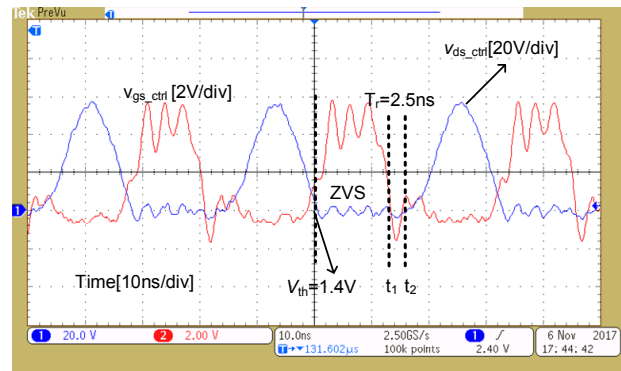
The prototype of the transformers including the front view and the side view are shown in Fig. 12. The proposed transformer is made up of two PCBs, with one-layer T1 at the top and three-layer T2 at the bottom. The insulated gaskets are placed between T1 and T2 to keep the required distance. Vernier caliper is used for measurements to make the spacing as close as possible to the design value. With the conventional transformer 0.60 mm thick and the proposed one 2.14 mm

thick, the small increase of thickness can be ignored compared with the thickness of the converter prototype 3.00 mm.

The waveforms of the eGaN control HEMT and SR in the converter with the proposed transformer with 15 V /24 W output are shown in Fig. 13. The MCU generates the driving signal of the control HEMT with a duty cycle of 51 %, as is shown in Fig. 13 (a). The control HEMT turns on just at the moment when the drain-to-source voltage  $v_{ds\_ctrl}$  resonates to zero. Then ZVS is achieved and the reverse conduction mechanism of the eGaN HEMT is not triggered. In Fig. 13 (b), the SR driving signal has a duty cycle of 40%. The SR turns on at the moment when the drain-to-source voltage  $v_{ds\_SR}$  resonates to zero and ZVS is also achieved. At  $t=t_1$ , the SR turns off and at  $t=t_2$ ,  $v_{ds\_SR}$  begins to resonate, so the reverse conduction mechanism is triggered. The SR has 2.5 ns reverse conduction time. The efficiency of the converter with the proposed transformer is up to 82.7% with 15 V input and 15 V/24 W output.



(a)  $v_{gs\_ctrl}$  and  $v_{ds\_ctrl}$



(b)  $v_{gs\_SR}$  and  $v_{ds\_SR}$

Fig. 13. Waveforms with proposed transformer:  $V_{in}=15$  V,  $V_{out}=15$  V,  $P_{out}=24$  W

The experimental thermal images are shown in Fig. 14 and Fig. 15. In the converter with the conventional transformer, With 15 V input and 15 V/21 W output, the control HEMT has a highest temperature of 89.4 °C, which prohibits further promotion of power. The transformer is slightly hot with a temperature of 51.7 °C. At the same output power, The proposed transformer has a temperature of 45.3 °C, which is a significant improvement compared with the conventional one.

Fig. 16 shows the loss distribution of the converter with two transformers at 15 V input and 15 V/21 W output. It is

observed that the major loss difference is the reverse conduction loss of  $S_r$  due to different reverse conduction time and the transformer loss. The loss of the proposed transformer is 1.83 W, a reduction of 0.80 W compared with the conventional transformer (2.63 W).

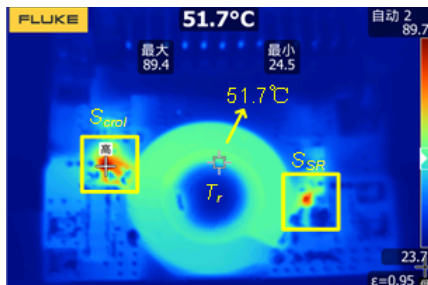


Fig. 14. Thermal image of conventional transformer:  $V_{in}=15\text{ V}$ ,  $V_{out}=15\text{ V}$ ,  $P_{out}=21\text{ W}$

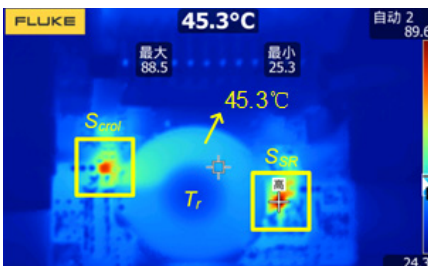


Fig. 15. Thermal image of proposed transformer:  $V_{in}=15\text{ V}$ ,  $V_{out}=15\text{ V}$ ,  $P_{out}=21\text{ W}$

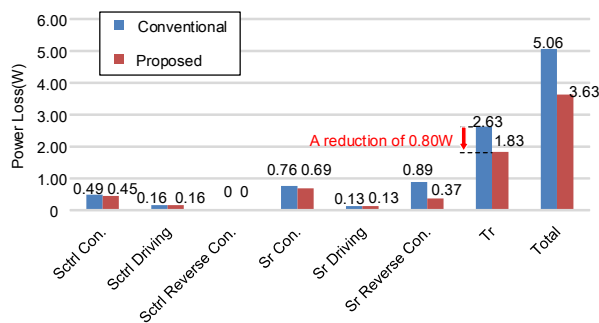


Fig. 16. Loss distribution:  $V_{in}=15\text{ V}$ ,  $V_{out}=15\text{ V}$ ,  $P_{out}=21\text{ W}$

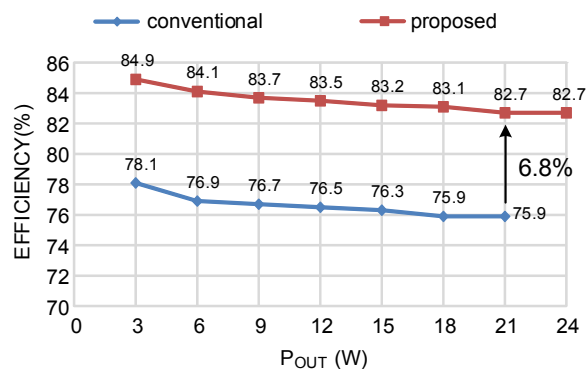


Fig. 17. Efficiency comparison curve:  $V_{in}=15\text{ V}$ ,  $V_{out}=15\text{ V}$ ,  $f=30\text{ MHz}$

The close-loop efficiency comparison ( $V_{in}=15\text{ V}$ ) under different output power is shown in Fig. 17. The efficiency curve drops with the increase of output power. One possible

reason is nonlinear variation of the frequency of ON/OFF control. The energy stored in the passive elements will be completely dissipated each time when the converter is shut off. The frequency of ON/OFF control improves with the increase of output power, which causes more energy dissipated. Another reason is that as the output power increases, the temperature of the eGaN HEMTs rises causing larger conduction resistance and more loss. With the low output power of 3W, the efficiency of the prototype is the highest, the conventional transformer 78.1% and the proposed transformer 84.9%. Under the input voltage of 15 V and the output of 15 V/21 W, the measured efficiency of the converter with the conventional transformer is 75.9%, while the measured efficiency of the converter with the proposed transformer is 82.7%. An efficiency improvement of 6.8% is achieved.

## V. CONCLUSION

A new helical air-core transformer structure with even current distribution is proposed for the VHF converters. The conventional helical air-core transformer suffers from serious eddy current loss caused by the proximity effect. The proposed helical transformer uses completely overlapped layers with the same geometry to constitute windings and adjusts the inductance value through changing the distance between layers. In this way, the flux path will not be shielded by the copper winding, which dramatically decreases the eddy current and improve the utilization of windings. Two transformers with similar parameters and different winding structures are designed and tested in VHF class E resonant flyback converters. The converter with the proposed transformer achieves an efficiency of 82.7% (15 V input, 15 V/21 W output) compared to 75.9% of the one with the conventional transformer (an improvement of 6.8%). With 24W output, the efficiency of converter with the proposed transformer is 82.7%. Through experimental verification, the proposed helical air-core transformer structure with even current distribution achieves higher efficiency. The new air-core transformer can be applied to other VHF converters with low power.

## REFERENCES

- [1] R. C. N. Pilawa-Podgurski, A. D. Sagneri, J. M. Rivas, D. I. Anderson, and D. J. Perreault, "Very high frequency resonant boost converter," *IEEE Trans. Power Electron.*, vol. 24, no. 6, pp. 1654-1665, 2009.
- [2] Z. Zhang, J. Lin, Y. Zhou, and X. Ren, "Analysis and decoupling design of a 30 MHz resonant SEPIC converter," *IEEE Trans. Power Electron.*, vol. 31, no. 6, pp. 4536-4548, 2016.
- [3] L. Gu, W. Liang, L. C. Raymond, and J. Rivas-Davila, "27.12 MHz GaN bi-directional resonant power converter," in *Proc. IEEE Workshop Control. Model. Power Electron.*, 2015, pp. 1-7.
- [4] Bouabana, Abdoukarim, C. Sourkounis, and M. Mallach. "Design and analysis of different structure of a coreless planar transformer for a flyback converter," *International Symposium on Power Electronics, Electrical Drives, Automation and Motion IEEE*, 2012:827-831.
- [5] A. D. Sagneri, D. I. Anderson and D. J. Perreault, "Transformer synthesis for VHF converters," *The 2010 International Power Electronics Conference - ECCE ASIA* -, Sapporo, 2010, pp. 2347-2353.
- [6] Bouabana, Abdoukarim, C. Sourkounis, and M. Mallach. "Design and analysis of different structure of a coreless planar transformer for a flyback converter," *International Symposium on Power Electronics, Electrical Drives, Automation and Motion IEEE*, 2012:827-831.
- [7] S. C. Tang, S. Y. Hui and Henry Shu-Hung Chung, "Coreless planar printed-circuit-board (PCB) transformers-a fundamental concept for

- signal and energy transfer," in *IEEE Transactions on Power Electronics*, vol. 15, no. 5, pp. 931-941, Sep 2000.
- [8] Z. L. Zhang, Z. Dong, X. W. Zou and X. Ren, "A Digital Adaptive Driving Scheme for eGaN HEMTs in VHF Converters," in *IEEE Transactions on Power Electronics*, vol. 32, no. 8, pp. 6197-6205, Aug. 2017.
- [9] A. D. Sagneri, "Design of miniaturized radio-frequency dc-dc power converters," Ph.D. dissertation, Dept. Elect. Eng. Comput. Sci., Massachusetts Inst. Technol., Cambridge, MA, USA, Feb. 2012.
- [10] W. G. Hurley and M. C. Duffy. "Calculation of self and mutual impedances in planar magnetic structures," *IEEE Transactions on Magnetics*, vol. 31, no. 4:2416-2422, 1995.